Model of diffusion on deformable lattices. III. Adatom-interaction effects

T. Ala-Nissila,* J. Kjoll, and S. C. Ying
Brown University, Department of Physics, Providence, Rhode Island 02912
(Received 15 October 1991; revised manuscript received 24 February 1992)

We present results of theoretical studies of diffusion in a lattice-gas model of a deformable lattice, which has been proposed to explain the anomalous diffusion anisotropy of H adatoms on a W(110) surface. In this work, we consider the effects of finite adatom-adatom interactions to diffusion in the model. In particular, using Monte Carlo simulation methods we study the properties of both tracer and collective diffusion in the presence of various spatially ordered phases within a model phase diagram of H/W(110). To incorporate the role of the energy barriers associated with diffusion more realistically, we select carefully a choice for transition probabilities used within the Monte Carlo method. We demonstrate that while the tracer and collective diffusion tensors behave in a fundamentally different manner within the model, the corresponding diffusion anisotropies are similar and are mainly controlled by the symmetry of the adlayer phase.

I. INTRODUCTION

One of the simplest example of a diffusive process consists of a classical particle executing isotropic random walk on an inert lattice. In the case of only one particle, its diffusion constant can be written down as va^2/z, where z is the coordination number of the lattice, v is the (microscopic) jump rate, and a the lattice constant (i.e., the length of each jump).[1] However, if any particle-particle interactions are present in the system the diffusion process becomes correlated, and a distinction has to be made between single particle or tracer, and collective diffusion processes.[2] A substantial amount of analytic work and numerical simulations have been done in simple model systems in order to study these correlation effects.[1-25] So far, accurate analytic solutions have been obtained in cases where only hard-core on-site exclusion interactions between particles exist.[2,18,19,23,24]

Surface diffusion of adatoms on substrates[26,27] provides an important realization of classical diffusion in two dimensions, and has frequently been modeled by lattice-gas systems.[2-25] However, modeling of surface systems involves two main complications. First, in real surface systems there are nonnegligible adatom-adatom interactions, which often dominate the behavior of adsorbates at low temperatures.[26,27] Second, in reality the adsorption of an adatom is often accompanied by a local substrate relaxation or distortion.[20-24] Recently, it has been proposed that this local distortion can have significant effect on the surface diffusion tensor.[20-24] In our previous works[22-24] in this series [hereafter referred to as I (Ref. 23) and II (Ref. 24)], a lattice-gas model was introduced that incorporates the essence of such a distortion with respect to diffusion. This model has originally been proposed[22] to explain the observed diffusion anisotropy of H adatoms on a W(110) surface.[20] The essence of the model is to recognize that the binding energy of an H adatom can be lowered if it is displaced locally from the original adsorption site along the $[1\bar{1}0]$ direction and accompanied by a shift of the surrounding substrate atoms in the same direction (see Fig. 1 of I). Obviously, the same is true if the displacements of both the adatom and the surrounding substrate atoms are reversed. This results in a "dynamical" double-well-type adsorption potential, which is imposed on the surface unit cell by each diffusing particle. The generation of such a double-well potential through a lattice distortion has been explicitly demonstrated in a previous work.[28] When the local distortions start to mutually correlate for higher coverages, a global surface reconstruction may occur, such as has been observed for H on W(110) around $c \gtrsim 0.5$.[29,30]

An important feature of the model is that even without direct adatom interactions, double occupation of an adsorption site is not favorable. This is due to the fact that a simultaneous occupation of the subsites leads to opposing surface relaxations which cancel each other, resulting in a much higher value of the total energy.[22] Since the time scale for the adatom motion is much longer than a typical time scale for the substrate response, the effect just described can be approximately modeled by splitting the original single adsorption site into *two* symmetric sites. When this is done, an energy barrier exists for the motion from one subsite to another. Moreover, a simultaneous occupation of the two subsites is then forbidden, i.e., a hard-core repulsion applies within each *cell*. Note that this is different from a true static "double-well" configuration as obtained in a previous model calculation.[31] For such a static well, double occupation of the subsites is possible provided that there are no strong direct repulsive interactions between the H adatoms. For the H/W(110) system, the hydrogen-induced distortion is more plausible because it provides a natural explanation for the global surface reconstruction at higher coverages.[22] In the context of a simple random-walk theory, the diffusive motion of the adatoms can then be considered to consist of two separate steps on a static lattice. The first is an *intracell* jump across the barrier originating from the local distortion, while the second is an *intercell* jump across the barrier due to the usual periodic arrangement of the substrate atoms. the competition be-

tween these two processes can be parametrized by a *branching ratio r,* which is the ratio of the intracell to intercell diffusion rates. An important point to note here is that from these simplifications it follows that this model is applicable to H/W(110) *only* in the regime $c \lesssim 0.5$ where no global surface reconstruction occurs.

In I and II, we present a detailed theoretical study of both tracer and collective diffusion processes within the lattice-gas model, assuming only hard-core interactions as described above. We demonstrate that the presence of both intracell and intercell jumps as well as the exclusion of double occupancy within a cell lead to a very complicated coverage dependence and cause strong correlation effects to appear. Remarkably enough, for the physically interesting case of $r \gtrsim 1$, the *diffusion anisotropy* displays universal behavior, in the sense that it is very similar for both tracer and collective diffusion. This is clearly due to the absence of broken-symmetry phases in the model with hard-core interactions only. However, as we have mentioned above, in realistic adsorption systems such as H/W(110), additional direct or indirect interactions exist between adatoms on different adsorption sites, as evidenced by the appearance of many distinct ordered phases of the adlayer.[29,30] Thus, it is of great importance to determine how the diffusion anisotropy is affected by the presence of such ordered phases.

In this work, we have undertaken a comprehensive numerical study of the effects of adatom-adatom interactions and ordered phases to diffusion within our lattice-gas model. We demonstrate how the presence of two distinct diffusion jumps leads to a somewhat unphysical dependence of diffusion on the form of the transition probability used in the standard Monte Carlo (MC) algorithm. To incorporate the role of the energy barriers in the model more realistically, we introduce a form for the transition probabilities used within the MC algorithm which is then compared with the standard forms. In particular, we demonstrate that although the absolute values of the diffusion coefficients depend on the choice of the MC algorithm, the *diffusion anisotropy* nevertheless remains virtually independent of the particular form of the transition probability used, and depends mostly on the global symmetry of the underlying phase.

The actual simulations in this work were done for a model with two sets of adatom interaction parameters. The first set is a model with nearest-neighbor interactions only, intended for a qualitative comparison with the hard-core interaction case. The second set is the lattice-gas model of Sahu *et al.*,[30] which they used to study the adsorption system H/W(110) in various parts of its phase diagram. This simplified model excludes the surface reconstruction of the W(110) substrate at $c \gtrsim 0.5$; however, the experimentally observed ordered phases formed by H are reproduced. Thus, our results may not be applicable to H/W(110) at higher coverages. We nevertheless present results of extensive Monte Carlo simulations of collective and tracer diffusion for all coverages, using mostly $r=3$, which for the hard-core interaction case most closely reproduces the experimentally observed diffusion anisotropy.[20,22]

II. MONTE CARLO SIMULATIONS OF DIFFUSION

As discussed in the Introduction, the physical motivation behind the diffusion model introduced by Kjoll *et al.*[22] is based on the anomalous diffusion anisotropy of H adatoms on a W(110) surface.[20] On an ideal surface, the underlying surface forms a centered rectangular lattice, with adatoms adsorbed on the long bridges sites within the "hourglass" potential [see Fig. 1(a) of I]. The principal axes of diffusion are given by the $[1\bar{1}0]$ and [001] directions denoted by y and x, respectively. When H is adsorbed on the surface, this local symmetry breaking is described by a *two-step lattice-gas model* with jump rates M and I for intracell and intercell rates, respectively, as shown in Fig. 1(c) of I. The branching ratio $r=M/I$ then determines the value of the diffusion anisotropy ratio, which in the zero coverage limit is given exactly by[22]

$$\frac{D_{yy}}{D_{xx}} = \frac{r}{r+2}\left[\frac{b}{a}\right]^2 . \tag{2.1}$$

Here a and b denote the dimensions of the underlying unit cell, and for the W(110) surface, $(b/a)^2=2$. By symmetry, the off-diagonal terms $D_{xy}=D_{yx}=0$.

For finite coverages, the simple result (2.1) for the anisotropy no longer holds. We must also distinguish between the behavior of the collective diffusion tensor D^c, and its tracer diffusion counterpart D^t. In I and II, assuming only hard-core interactions within each cell, we were able to analytically calculate both D^c and D^t using the Green's function method of Tahir-Kheli and Elliott.[18,19] For branching ratios $r \gtrsim 1$, the results were in rather good agreement with corresponding MC simulations. Most remarkably, for such larger values of r the anisotropy ratio is well described by a nontrivial mean-field theory associated with the Green's function method. which gives:[23,24]

$$\frac{D^t_{yy}}{D^t_{xx}} = \frac{D^c_{yy}}{D^c_{xx}} = \frac{r}{r+2v}\left[\frac{b}{a}\right]^2 , \tag{2.2}$$

where $v=1-c$ is the vacancy factor. In particular, (2.2) reveals that either in the limit $r\to\infty$, where the effect of the local distortion vanishes or in the limit $c\to 1$, the diffusion anisotropy (2.1) approaches the value of 2, appropriate for a simple lattice-gas model of undistorted W(110).[20] Also, for any finite value of r and $c<1$, the anisotropy ratio is always less than 2 in accordance with experiments of H diffusion.[20] However, when finite adatom-adatom interactions are introduced in the two-step model, the analytic solutions for the collective and tracer diffusion are no longer valid, except in the trivial limits of very high temperatures $k_BT\to\infty$, or $c\to 0$. The transition rates I and M become explicitly dependent both on interactions and local configurations. Because of the lack of an analytic theory, we must resort to MC simulations to study diffusion at finite coverages and, in particular, the diffusion anisotropy in the presence of interactions. Before presenting the results of our simula-

tions, we discuss below the role of the transition probabilities in determining the coverage and temperature dependence of diffusion coefficients in the model.

A. Choice of transition probabilities

Aside from the usual problem of the interpretation of the dynamics in the Metropolis Monte Carlo method,[32] there is an additional ambiguity associated with the choice of the transition probabilities when time-dependent phenomena such as diffusion are simulated.[9,15,32] Namely, the condition of microscopic reversibility,

$$w_{i,f}p_i = w_{f,i}p_f \ , \tag{2.3}$$

where $w_{i,f}$ is the transition rate from a state $\langle i \rangle$ to a state $\langle f \rangle$, and p_i and p_f are corresponding probability densities, does not specify the transition rates uniquely. Two of the most commonly used functional forms for the rates are the Metropolis form[33]

$$w_{i,f} = \begin{cases} \nu e^{-\beta \Delta E}, & \text{if } \Delta E > 0 \ , \\ \nu, & \text{if } \Delta E \le 0 \end{cases} \tag{2.4}$$

and the symmetric Kawasaki form[34]

$$w_{i,f} = \tfrac{1}{2}\nu[1-\tanh(\tfrac{1}{2}\beta \Delta E)] \ , \tag{2.5}$$

where $\Delta E \equiv E_f - E_i$ is the energy difference between the final and initial states, ν is the attempt frequency, and $\beta \equiv 1/(k_B T)$ is the inverse temperature. Usually, ν is set to unity and time is measured in units of transition attempts per particle.

In studying diffusion, either (2.4) or (2.5) can in principle be employed. Some studies have also been done using the exponential function in (2.4), but identifying $\Delta E = E_i$ as the initial-state energy instead of the energy difference.[21] An additional normalization factor including the maximum value of energy has to be included also. This choice is based on the activated nature of classical diffusion processes, and is sometimes called the "initial-value dynamics." However, the barrier introduced with this choice of transition probability is somewhat artificial. A second and more serious problem is that if the energy distribution is relatively wide, the initial-value dynamics becomes very inefficient at low temperatures. We should also note already at this point that the coverage dependence of diffusion is clearly rather sensitive to the choice of $w_{i,f}$. For example, the choice of the Kawasaki form (2.5) preserves particle-hole symmetry whereas the initial-value dynamics does not.

The fundamental problem with all these choices, including (2.4) and (2.5) is that they do not realistically describe the diffusion process in terms of an intermediate energy state, which for classical diffusion is the saddle point of the adiabatic surface potential.[35] This becomes particularly serious for our model. Namely, consider the intracell jumps, for which ΔE is always zero. This means that not only the absolute diffusion rates but also the *diffusion anisotropy* depend on the particular choice of the MC transition probabilities. However, in reality the intracell rate should be controlled by a saddle point within the cell, created by the local distortion [Fig. 1(c) in I]. In fact, microscopic calculations of single-particle diffusion in distorted potentials have demonstrated[28] that the temperature dependence of D and the anisotropy ratio are controlled by the relative magnitudes of *two* saddle points on the surface, located at L and S (Fig. 1 in I).

Since the dynamics of diffusion will always depend on the choice of the MC transition probabilities, we can actually utilize this freedom to more realistically model the diffusion process within the two-step model. To this end we have chosen a form of the transition probability in which the intracell and intercell diffusion jumps are decomposed into two steps, i.e.,

$$w_{i,f} = w_{i,s}w_{s,f} \ . \tag{2.6}$$

The first transition rate $w_{i,s}$ describes a transition from an initial energy state E_i to an intermediate energy state E_s, and it is given by

$$w_{i,s} = \tfrac{1}{2}\nu_1\{1-\tanh[\beta(E_s - E_i)/2]\} \ . \tag{2.7}$$

Similarly, the second transition rate describes a transition from the intermediate state to the final energy state E_f:

$$w_{s,f} = \tfrac{1}{2}\nu_2\{1-\tanh[\beta(E_f - E_s)/2]\} \ . \tag{2.8}$$

Thus, for both steps the transition probabilities have the familiar Kawasaki form, although (2.4) is also equally applicable. It is easy to verify that (2.6)–(2.8) satisfy the detailed balance condition, as required. Our choice of the transition probabilities describes explicitly the effect of an intermediate energy state in the diffusion process, which in the classical picture is the saddle point of the potential. We shall refer to this choice of probability of transition as the *transition dynamics algorithm* (TDA). Within the TDA, there is still a freedom of choice for the intermediate barrier E_s, which will be discussed in subsequent sections.

When applied to the two-step model, neither the rates ν_1 and ν_2 nor the saddle-point energies for the intercell and intracell jumps need to be identical. The definition of a "bare" one-particle branching ratio then becomes $r = (\nu_1\nu_2)^M/(\nu_1\nu_2)^I$, while the *effective* branching ratio r^{eff} is given by

$$r^{\text{eff}} \equiv \frac{w_{i,s}^M w_{s,f}^M}{w_{i,s}^I w_{s,f}^I} \ , \tag{2.9}$$

where I and M refer to intracell and intercell jumps, respectively. Note that only in the limit of an infinite temperature does (2.9) reduce to a constant similar to the cases discussed in I and II. In general, r^{eff} is temperature and coverage dependent and could even change with different configurations according to the choice of E_s.

B. Model with nearest-neighbor interactions

To study systematically the effects of finite interactions and the choice of different MC transition probabilities to diffusion in the two-step model, we have first performed simulations for a model of isotropic nearest-neighbor interactions given by

$$H=J\sum_{\langle gg'\rangle,ss'} n_g^s n_{g'}^{s'} . \tag{2.10}$$

As in I and II, g and g' are cell indices, s,s' refer to sublattices A and B, and $n's$ denote the usual lattice gas occupation variables. For the interaction between the adatoms, no distinction is being made between the "up" and "down" sites of the cells, and thus for half coverage $c=\frac{1}{2}$, (2.10) corresponds to the two-dimensional Ising model with a phase transition at $J/(4k_BT)\approx 0.4407$. For other coverages, the model Hamiltonian describes an Ising model in an external field.

We have studied collective and tracer diffusion in the case of both attractive and repulsive nearest-neighbor interactions. Here we first discuss our results for the case of tracer diffusion, which can then be directly compared with the results in II. To calculate the tracer diffusion coefficient, we have used the definition

$$D^t_{\alpha\alpha}=\frac{1}{N}\lim_{t\to\infty}\frac{1}{t}\sum_{i=1}^{N}\langle |R^i_\alpha(0)-R^i_\alpha(t)|^2\rangle, \quad \alpha=x,y, \tag{2.11}$$

where N is the number of particles, $R^i_\alpha(t)$ denotes the spatial component of the position vector of the ith particle at time t, and $\langle\ \rangle$ denotes configuration averaging. In the algorithm, each diffusing particle is tagged and the displacements are averaged over all of the N particles to improve statistics. Further details of the method used can be found in our previous work in II.

Comparisons of the effect of transition probabilities were done between the Kawasaki form, and the TDA in which we set $r=3$, with $E_s=\langle E\rangle$ for both intracell and intercell jumps. Analysis of tracer diffusion data for 60×60 systems was performed similarly to the case of hard-core interactions only. We checked the high-temperature limit of $B\to 0$ by running simulations at $\beta J=0.4$, which gave results essentially identical to that described in II. In Fig. 1 we first present results for the tracer-diffusion anisotropy D^t_{yy}/D^t_{xx} for the cases where $\beta J=1.428$, and $\beta J=-1.428$. At this temperature the

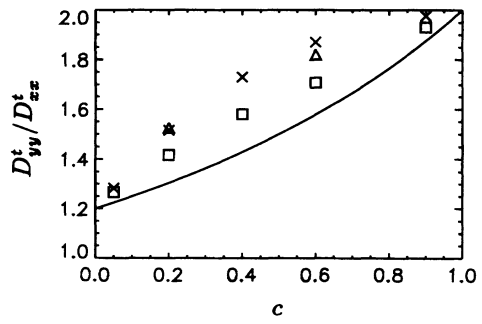

FIG. 1. Comparison of the tracer-diffusion anisotropy vs coverage for the nearest-neighbor lattice-gas model with Kawasaki dynamics ($\beta J=-1.428$, squares; $\beta J=1.428$, crosses) with the transition dynamics algorithm, where $E_s=\langle E\rangle$ (triangles for both repulsive and attractive cases). Error bars are about the size of the points, or smaller. For reference, the solid line indicates the mean field result (2.2).

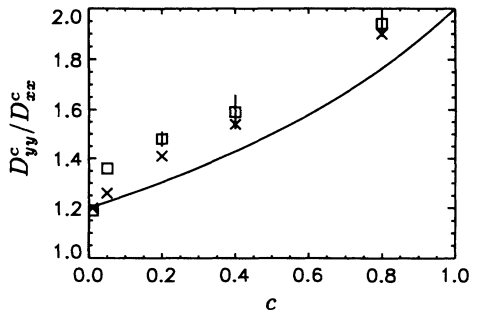

FIG. 2. Collective diffusion anisotropy vs coverage for the nearest-neighbor lattice-gas model, with $\beta J=-1.428$ (squares) and $\beta J=1.428$ (crosses). A strong critical slowing down of diffusion makes it difficult to determine D_{yy}/D_{xx} accurately for the case of attractive interactions, as indicated by the error bars. The mean field solution (2.2) is shown by a solid line.

corresponding Ising model is still disordered even for $c=\frac{1}{2}$, but for all coverages there is a considerable amount of local ordering present in the form of clusters. Our results show clearly that although the absolute diffusion rates are rather different from the hard-core case, and also depend strongly on the sign of J, the diffusion *anisotropy* is rather insensitive to either interactions or the transition probabilities used. For our particular choice of E_s, the results for TDA are close to the Kawasaki case. Using different values of E_s for intracell and intercell jumps one can definitely change the anisotropy ratio, but for any reasonable choices where the ratio E_s^M/E_s^I is not much different from unity, the effect is not very large. The main qualitative feature of the two-step model, the reduction of D_{yy}/D_{xx} from the value of 2, always manifests itself in the absence of spatially ordered phases.

In the case of collective diffusion, we observed a strong critical slowing down effect in the case of attractive interactions as expected from standard theoretical arguments,[36] while for the repulsive case no such anomalous temperature dependence was observed. Analogous results have also been obtained by Jiang and Methiu[14] in their MC study of the Ising model on a square lattice. In Fig. 2, we display the anisotropy ratio D^c_{yy}/D^c_{xx} as a function of coverage, calculated using Kawasaki dynamics. Both D^c_{xx} and D^c_{yy} were calculated from the density fluctuation autocorrelation function, as explained in I. The same conclusions as above apply to the case of collective diffusion. Again, the diffusion anisotropy behaves in a manner very similar to that in I.

III. MODEL OF H/W(110) WITH FULL INTERACTION PARAMETERS

In this section, we describe the simulation results for our two-step lattice-gas model in which the interaction parameters are taken from a recent study by Sahu *et al.*[30] on the H/W(110) adsorption system. This model makes no allowance for a local distortion or surface reconstruction but the direct H-H interactions are chosen such that the experimentally observed phase diagram of H/W(110) is correctly reproduced. Thus, it should provide a good

description for H/W(110) at least for $c < \frac{1}{2}$ before the global surface reconstruction takes place. Again, we make the simplifying assumption that interaction between the hydrogen atoms does not depend on which sublattice they are on (i.e., on A or B), but only on the separation between the cells. The interaction Hamiltonian is therefore given by

$$H = \sum_{\langle gg' \rangle, ss'} J(g,g') n_g^s n_{g'}^{s'} . \tag{3.1}$$

Here $s,s' = A$ or B, and g,g' denote the cell indices. The interaction parameters are chosen such[30] that $J_1 = -1$, $J_2 = J_3 = -\frac{1}{2}$, $J_4 = -1$, and $J_{t1} = J_{t2} = 0.6$, and their meaning is illustrated in Fig. 3(a). In Fig. 3(b) we show the phase diagram of the model, as calculated by Sahu *et al.*[30]

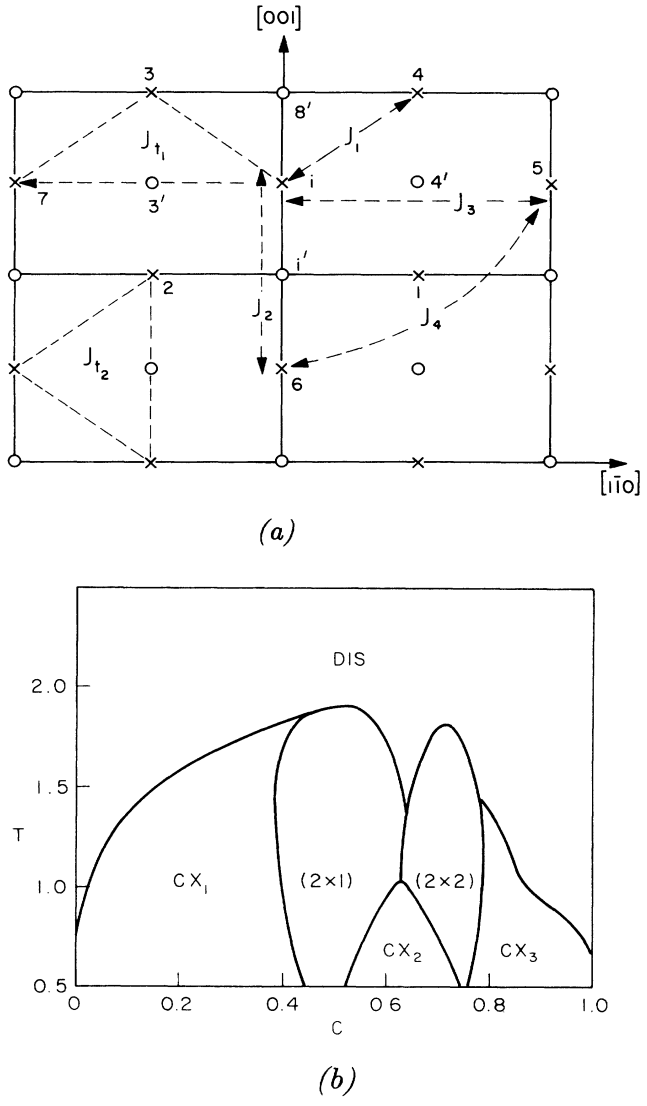

FIG. 3. (a) A schematic figure of the interaction parameters used in the model of H/W(110) (from Ref. 30). Crosses denote the positions of the hourglass adsorption sites for H. (b) The corresponding model phase diagram for H/W(110). CX_i's denote coexistence regions between different phases (from Ref. 30).

Our simulations of diffusion were carried out using the TDA exclusively. The intermediate "barrier" energy parameter E_s was chosen to be

$$E_s = \frac{E_i + E_f}{2} + \Delta . \tag{3.2}$$

The first term in (3.2) is an approximate representation of the interaction energy with other adsorbates when the atom making the jump is at the "transition state." The quantity Δ represents the intrinsic saddle-point barrier, and in most runs we set $\Delta = 0.5$ in the same units as the interaction parameters.[37] For the results presented below, the bare branching ratio r was set to three. Note that with this choice of E_s, r^{eff} in (2.10) is not only temperature dependent but also a running variable in the MC simulations since E_s changes with configurations.

Typically, the diffusion constants are extracted from runs up to 600 MC steps, using 60×60 or 30×30 systems. However, a large number $(10^3 - 10^4)$ of configuration averages is required to obtain accurate data. The independence of initial configurations, which must be carefully equilibrated, is achieved by randomizing the configurations using long multisite diffusion jumps for the adatoms.

A. Tracer diffusion

We shall first describe the results for the coverage dependence of the tracer-diffusion tensor D^t. At the temperature $T = 1.5$, according to the phase diagram in Fig. 3(b), the adsorbate will form a (2×1) [or (1×2)] ordered phase around $c = \frac{1}{2}$ and a (2×2) phase around $c = \frac{3}{4}$. In Figs. 4(a) and 4(b) we present results for D_{xx}^t, D_{yy}^t, and D_{xy}^t as a function of coverage at $T = 1.5$. The first feature to note is that the diffusion constants drop off much more rapidly as a function of coverage compared with the hard-core interaction case in II. This is because of the fact that, besides the blocking factor which increases as the coverage increases, a well-ordered local environment for the diffusing adatom means that any jump leading to a different configuration will necessarily involve a large activation energy, hence leading to a smaller diffusion constant. Using this simple argument, we also expect the diffusion constants D_{xx}^t and D_{yy}^t to show a local minimum at $c = \frac{1}{2}$ and $c = \frac{3}{4}$, which correspond to the maximal ordering of the (2×1) and (2×2) phases, respectively. This is precisely the case as seen in Figs. 4(a) and 4(b). The behavior of the off-diagonal component of the diffusion tensor D_{xy}^t on the other hand is rather different. It is zero at most values of the coverage but becomes finite around $c = \frac{1}{2}$ where it displays a local maximum. The reason for this is that D_{xy}^t is a measure of the symmetry of the diffusion behavior. For the disordered phase and the (2×2) phase, the principal axes of diffusion are just along the x and y axes of the lattice. However, in the (2×1) or the (1×2) phase, diffusion is obviously taking place mainly along the direction of the occupied rows, as shown schematically in Fig. 5. Thus the nonzero value of

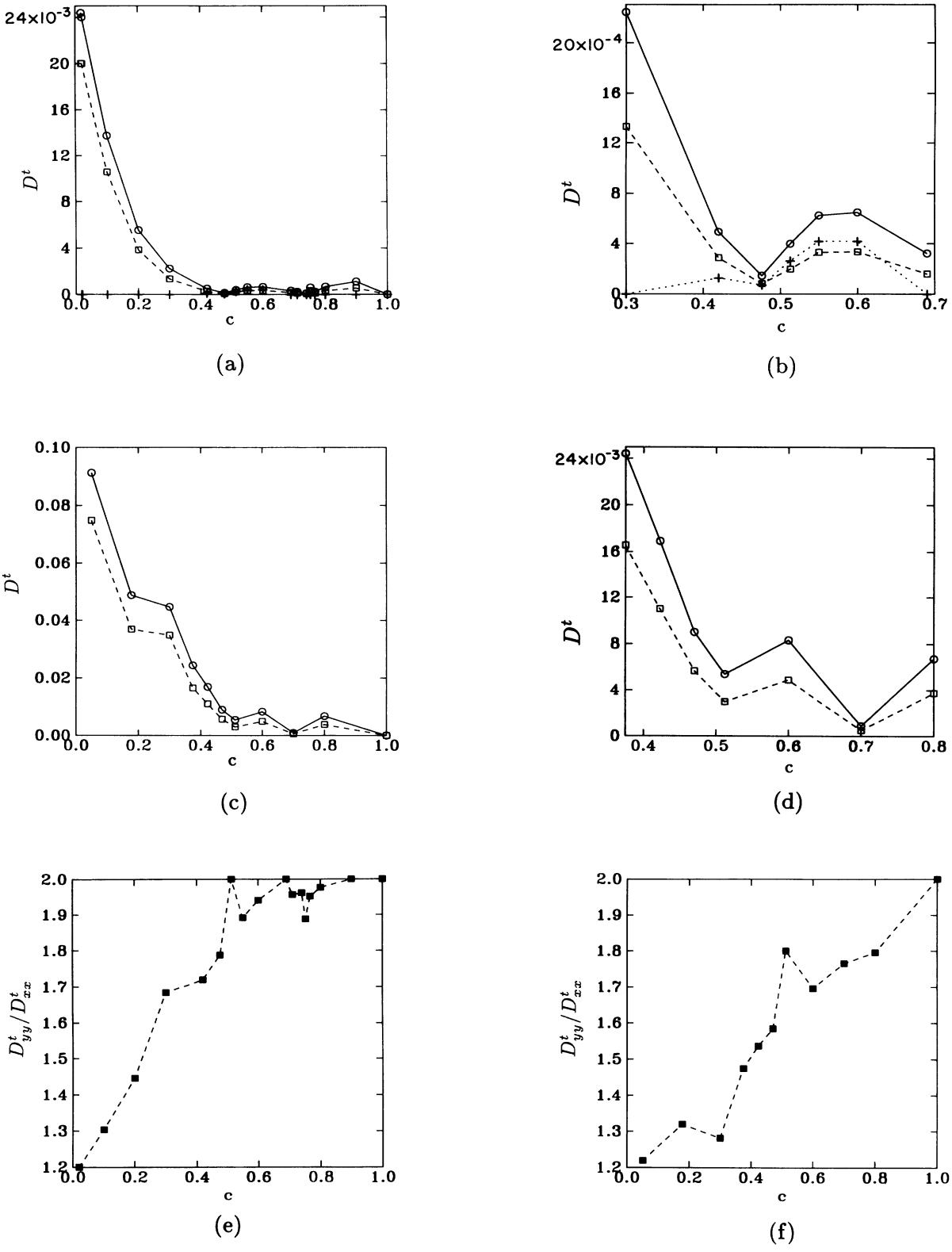

FIG. 4. (a) Coverage dependence of D^t_{xx} (squares), D^t_{yy} (circles), and D^t_{xy} (crosses) for the model of H/W(110) at $T=1.5$, in units of $2a^2\nu$, $b^2\nu$, and $b^2\nu$, respectively, where $2a^2=b^2$ and ν is an arbitrary rate constant (cf. Refs. 23 and 24). (b) Details for intermediate coverages. Lines are only guides to the eye. (c) and (d) Coverage dependence of D^t_{xx} (squares) and D^t_{yy} (circles) for the model of H/W(110) at $T=2.2$. D^t_{xy} is now virtually zero, as the global order is very weak. (e) Tracer diffusion anisotropy corresponding to (a); (f) Tracer-diffusion anisotropy corresponding to (c).

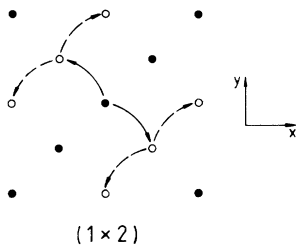

FIG. 5. Figure showing, schematically, how in a fully ordered (1×2) [(2×1)] phase the particles (filled circles) can only move diagonally along the empty rows of adsorption sites (open circles). This leads to a rotation of the principal axes for diffusion and a finite D_{xy}, as discussed in the text.

D^t_{xy} around $c=\frac{1}{2}$ simply indicates that the principal axes of diffusion at those coverages are rotated from their original direction.

At a higher temperature $T=2.2$, the phase diagram in Fig. 3(b) indicates that there are no more ordered phases at any coverages. However, this result is for the infinite size limit, as obtained from finite-size-scaling studies.[30] For the actual 30×30 system studied here, the adsorbate layer is still in a weakly ordered (2×1) [or (1×2)] phase around $c=\frac{1}{2}$. Thus the diffusion constants D^t_{xx} and D^t_{yy} still have weak local maxima at $c=\frac{1}{2}$ as shown in Figs. 4(c) and 4(d). The local maximum at $c=\frac{3}{4}$, however, has almost completely disappeared because the (2×2) phase is disordered at this temperature.

In Figs. 4(e) and 4(f) we show the anisotropy ratios D^t_{yy}/D^t_{xx} for these two temperatures. As expected from the above discussions, the result for $T=2.2$ is very similar to the case of hard-core interactions only, except for the peak at $c=\frac{1}{2}$ arising from the weak remnant of the (2×1) [or (1×2)] phase. For the lower temperature of $T=1.5$, the ratio rises rapidly towards the asymptotic value of 2 for $c>0.5$. This is due to the large activation energies in the ordered phases for the intercell jumps, as opposed to intracell jumps which are controlled only by the intrinsic saddle-point barrier. The effective branching ratio r therefore rises rapidly. Since the anisotropy ratio becomes two in the limit where r approaches infinity, this gives rise to the observed behavior of the rapid rise of the anisotropy ratio as a function of coverage at lower temperatures.

B. Collective diffusion

The collective diffusion tensor D^c is evaluated by studying the long time decay of the density-density correlation functions as done in I. Again we show results for the two temperatures $T=1.5$ [Figs. (6(a) and 6(b)] and $T=2.2$ [Fig. 6(c)]. There are two major qualitative differences when compared with the corresponding results for the tracer diffusion. First, the collective diffusion falls off much more slowly as a function of coverage. This is not unexpected because the success rate of a single adatom jump event is not the sole factor in determining the rate of collective diffusion. In fact, the results in I for the simple hard-core interaction model already indicate a very weak dependence of the collective diffusion tensor on the coverage. The second major difference is that the collective diffusion rises to a local maximum instead of a minimum at $c=\frac{1}{2}$ and $c=\frac{3}{4}$ where the adlayer is in the (2×1) [or (1×2)] and (2×2) phases, respectively. This can be seen clearly in the case where $T=1.5$. For $T=2.2$, the local maximum persists at $c=\frac{1}{2}$ but disappears at $c=\frac{3}{4}$. This is again due to the disordering of the (2×2) phase at this higher temperature. The reason for this behavior can be best understood from the phenomenological expression relating the collective diffusion to an effective jump frequency $\nu(c)$ of single particles:[7,27]

$$D^c=\frac{1}{4}\nu(c)a^2\frac{1}{k_BT\rho\kappa}\ , \tag{3.3}$$

where ρ is the density and κ is the adlayer compressibility. In this expression, the numerator is obviously minimized at $c=\frac{1}{2}$ and $c=\frac{3}{4}$ because the single adatom jump success rate is lowest for the fully ordered (2×1) [or (1×2)] and (2×2) phases. However, the denominator contains the compressibility κ, which displays a minimum at the fully ordered phases of the adlayer. Thus, there is a competition between these two factors. For the model system studied here, the compressibility is the dominant factor and thus the diffusion constants acquire a maximum at $c=\frac{1}{2}$ and $c=\frac{3}{4}$. This kind of behavior has indeed been observed experimentally in such systems as Li/W(110) and Ba/Mo(011).[26] For other systems, the situation could be reversed.[38] For example, in the simulation studies of Sadiq and Binder,[9] they observe a minimum instead of a maximum for the collective diffusion at a fully ordered phase.

The off-diagonal element D^c_{xy} shows a behavior similar to the tracer-diffusion case. This is to be expected because the principal axes of the collective diffusion tensor should be identical to those of the tracer-diffusion tensor. Finally, the anisotropy ratio D^c_{yy}/D^c_{xx} for low coverages is similar to that for tracer diffusion, as can be seen in Fig. 6(d). In the higher temperature of $T=2.2$, the ratio again displays a weak peak around $c=\frac{1}{2}$, beyond which it drops off before rising to its eventual limit of $D^c_{yy}/D^c_{xx}=2$.

IV. DISCUSSION AND CONCLUSIONS

In this work, we have complemented our previous theoretical studies of diffusion[22–24] in a lattice-gas model of a deformable lattice, by considering the influence of finite adatom interactions. Because of the lack of an analytic theory, we have resorted to Monte Carlo simulations to study the coverage dependence of D^t and D^c. To more realistically incorporate the role of saddle points controlling diffusion, we have used a form of the transition probabilities within the Monte Carlo method. Using this approach, we have performed extensive simulations of both tracer and collective diffusion in a model of H/W(110) with full interaction parameters. Our results demonstrate clearly the influence of the ordered adlayer phases to diffusion, and also delineate the fundamentally different nature of tracer and collective diffusion in in-

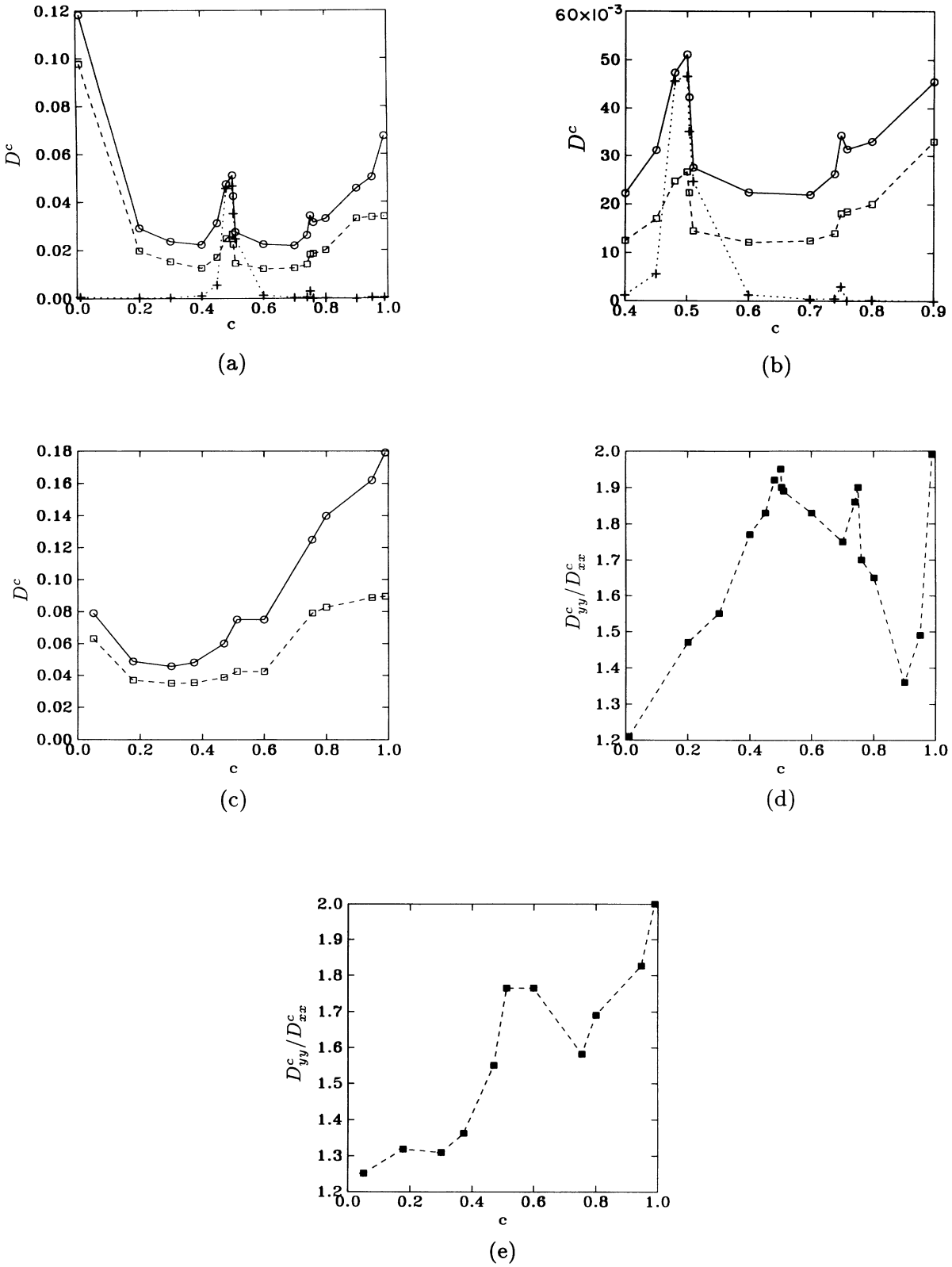

FIG. 6. (a) Coverage dependence of D^c_{xx} (squares), D^c_{yy} (circles), and D^c_{xy} (crosses) for the model of H/W(110) at $T=1.5$. Units are as in Fig. 4. (b) Details for intermediate coverages. Lines are only guides to the eye. (c) Coverage dependence of D^c_{xx} (squares) and D^c_{yy} (circles) for the model of H/W(110) at $T=2.2$. D^c_{xy} is again zero at this higher temperature. (d) Collective diffusion anisotropy corresponding to (a). (e) Collective diffusion anisotropy corresponding to (c).

teracting systems. Most strikingly, for our model, tracer diffusion shows pronounced *minima* for maximal ordering as a function of coverage while the collective diffusion displays local *maxima* for the same values of c. This difference can be qualitatively explained by the difference between adatom mobilities and the compressibility of the adlayer.

Despite the well-known fact that Monte Carlo studies cannot be used to quantitatively estimate diffusion coefficients in real interacting systems, we believe that at least the *qualitative* features of our model should apply to H/W(110) for $c<0.5$. Most importantly, our work demonstrates that the *diffusion anisotropy ratios* D_{yy}^t/D_{xx}^t and D_{yy}^c/D_{xx}^c behave in a very similar fashion and are mostly determined by the global symmetry of the adlayer. The anisotropy is also rather sensitive to the degree of local ordering, as demonstrated by our high-temperature results in Sec. III. The temperature dependence of the anisotropy is also sensitive to the ratio of the intracell barrier Δ_I to the intercell barrier Δ_M. In this work we have set $\Delta_I/\Delta_M=1$ for lack of microscopic information.[37] Within the model, the diffusion anisotropies are always less than 2, except at low temperatures where long-range order in the adlayer emerges. These results are consistent with the current experiments[20,27] on the anisotropy of collective diffusion in H/W(110).

ACKNOWLEDGMENTS

This work is supported by an ONR contract. We also want to thank the National Center for Supercomputing Applications at the University of Illinois at Urbana-Champaign for an allocation of supercomputer time.

*Present address: Research Institute for Theoretical Physics, University of Helsinki, Siltavuorenpenger 20 C, SF-00170 Helsinki, and Tampere University of Technology, Department of Physics, SF-33101 Tampere, Finland.

[1]See, e.g, K. W. Kehr, R. Kutner, and K. Binder, Phys. Rev. B **23**, 4391 (1981).

[2]K. W. Kehr and K. Binder, in *Applications of the Monte Carlo Method in Statistical Physics,* edited by K. Binder (Springer-Verlag, New York, 1987), p. 181 and references therein.

[3]J. P. Van der Eerden, D. Kashhiev, and P. Bennema, J. Cryst. Growth **42**, 31 (1977).

[4]M. Bowker and D. King, Surface Sci. **71**, 583 (1978); **72**, 208 (1978).

[5]H. Aasada and M. Masuda, Surface Sci. **99**, L429 (1980).

[6]G. E. Murch, Phil. Mag. A **43**, 871 (1981).

[7]D. A. Reed and G. Erlich, Surface Sci. **102**, 588 (1981).

[8]T. T. Tsong, Surface Sci. **122**, 99 (1982).

[9]A. Sadiq and K. Binder, Surface Sci. **128**, 350 (1983).

[10]M. Tringides and R. Gomer, Surface Sci. **145**, 121 (1984).

[11]A. Natori and H. Ohtsubo, Surface Sci. **171**, 13 (1986); **184**, 289 (1987).

[12]C. H. Mak, J. L. Brand, B. G. Koehler, and S. M. George, Surface Sci. **191**, 108 (1987).

[13]C. H. Mak, H. C. Andersen, and S. M. George, J. Chem. Phys. **88**, 4052 (1988).

[14]X.-P. Jiang and H. Methiu, J. Chem. Phys. **88**, 1891 (1988).

[15]H. C. Kang and W. H. Weinberg, J. Chem. Phys. **90**, 2824 (1989).

[16]L. A. Ray, R. C. Baetzold, and J. Simon, Surface Sci. **235**, 47 (1990).

[17]M. V. Arena, A. A. Deckert, and S. M. George, Surface Sci. **241**, 369 (1991).

[18]R. A. Tahir-Kheli and R. J. Elliot, Phys. Rev. B **27**, 844 (1983).

[19]R. A. Tahir-Kheli, Phys. Rev. B **27**, 6072 (1983); R. A. Tahir-Kheli and N. El-Meshad, Phys. Rev. B **32**, 6166 (1985).

[20]M. Tringides and R. Gomer, Surface Sci. **155**, 254 (1985).

[21]M. Tringides and R. Gomer, Surface Sci. **166**, 419 (1986); **166**, 440 (1986).

[22]J. Kjoll, T. Ala-Nissila, and S. C. Ying, Surface Sci. **218**, L476 (1989).

[23]T. Ala-Nissila, J. Kjoll, S. C. Ying, and R. A. Tahir-Kheli, Phys. Rev. B **44**, 2122 (1991).

[24]T. Ala-Nissila, J. Kjoll, S. C. Ying, and R. A. Tahir-Kheli, Phys. Rev. B **44**, 2133 (1991).

[25]Yu. K. Tovbin, Prog. Surface Sci. **34**, 1 (1990).

[26]A. G. Naumovets and Yu. S. Vedula, Surface Sci. Rep. **4**, 365 (1985).

[27]R. Gomer, Rep. Prog. Phys. **53**, 917 (1990).

[28]T. Ala-Nissila and S. C. Ying, Surface Sci. Lett. **235**, L341 (1990).

[29]J. W. Chung, P. Estrup, and S. C. Ying, Phys. Rev. Lett. **56**, 749 (1986).

[30]D. Sahu, J. M. Kosterlitz, and S. C. Ying, in *The Structure of Surfaces II,* edited by J. F. Van der Veer and M. A. Van Hove (Springer-Verlag, New York, 1988).

[31]P. Nordlander, S. Holloway, and T. K. Norskov, Surface Sci. **136**, 59 (1984).

[32]K. Binder, in *Monte Carlo Methods in Statistical Physics,* edited by K. Binder (Springer-Verlag, New York, 1979), p. 1; K. Binder and D. Stauffer, in *Applications of the Monte Carlo Method in Statistical Physics,* Ref. 2, p. 1.

[33]M. Metropolis, A. W. Rosenbluth, M. N. Rosenbluth, A. N. Teller, and E. Teller, J. Chem. Phys. **21**, 1087 (1953).

[34]K. Kawasaki, Phys. Rev. **145**, B224 (1966); **148**, 375 (1966); **150**, 285 (1966).

[35]T. Ala-Nissila and S. C. Ying, Phys. Rev. Lett. **65**, 879 (1990); T. Ala-Nissila and S. C. Ying, Phys. Rev. B. **42**, 10264 (1990).

[36]G. Mazenko, in *Surface Mobilities on Solid Materials,* edited by V. T. Binh (Plenum, New York, 1983).

[37]Note that since the experimental estimate for the intercell barrier Δ_M is about 2000 K and the interaction parameters are about 300 K, the barriers chosen in this work are probably lower than in reality. However, for the purpose of studying the anisotropy, only the barrier ratios are relevant. In either circumstance, the quantum tunneling effects of H atoms are totally negligible at room temperature.

[38]A. G. Naumovets, V. V. Poplovsky, and Yu. S. Vedula, Surface Sci. **200**, 321 (1988); T.-S. Lin, H.-J. Lu, and R. Gomer, Surface Sci. **234**, 251 (1990).